Artificial pneumatic cilia

B. Gorissen[a,*], E. Milana[a], M. De Volder[a,b] and D. Reynaerts[a]

[a] Department of Mechanical Engineering, KULeuven, Celestijnenlaan 300, 3001 Heverlee, Belgium

[b] Institute for Manufacturing, University of Cambridge, 17 Charles Babbage Road, Cambridge CB3 0FS, UK

[*] Corresponding author: benjamin.gorissen@kuleuven.be

1. INTRODUCTION

Well hidden from the macroscopic view of the human eye lays the fascinating word of low Reynolds fluid flow. This world is vastly different from the moderate to high Reynolds numbers that we encounter in our daily lives. Where the reciprocal motion of a fish's tail fin is an excellent mechanism for achieving fluid flow at Re>1, a low Reynolds fish wouldn't be able to advance using the same motion. Nature's evolutionary mechanism devised some unique solutions to the low Reynolds number fluid propulsion problem, such as vibrating hair like structures that beat in an orchestrated pattern, called cilia. Due to the small dimensions of these cilia, they almost exclusively operate at low Reynolds number, where asymmetry is essential to achieve net propulsion. This is best known as the Scallop theorem that states that a low Reynolds swimmer must deform in a way that is not invariant under time-reversal [1].

These asymmetrically moving cilia are difficult to mimic at a microscale using devices made by traditional fabrication processes. However, with the advent of micro- and nanotechnology, we now have a set of new tools to better imitate the propulsion of biologic microorganisms. The main challenge consists of developing artificial cilia that exhibits all types of asymmetry that natural cilia display, while having roughly the same size. In nature, four types of ciliary asymmetry are found. Three of them act on the level of a single cilium [2]: spatial asymmetry, where effective and recovery strokes do not follow the same path; orientational asymmetry, where the mean axis of the cilium is spatially tilted away from the surface normal; and temporal asymmetry where effective and recovery strokes have different velocities. At the level of the cilia array as a whole, additional asymmetry can be created by generating metachronal waves where a phase difference in actuation is present between neighbouring cilia [3]. Although spatial asymmetry is a necessary boundary condition to achieve low Reynolds fluid flow, cilia in nature usually combine different types of asymmetry to form complex beating patterns in order to maximize fluid propulsion [4]. In the past decade, advanced artificial cilia were developed that exhibit multiple asymmetry modes, using different actuation technologies, with performances that match those of natural cilia. An overview of artificial cilia described in literature can be found in table 1, where the actuation principle is used to classify them, together with achieved asymmetry and cilium length. Since temporal asymmetry has no influence on low Reynolds fluid flow, it has been omitted in the table.

Table 1 Overview of artificial cilia in literature

Actuation Principle	Asymmetry Type			Cilium Length [μm]	Reference
	Spatial	Orientational	Metachronal		
Magnetic	yes	yes	no	10-25	[5, 6]
	yes	yes	no	300	[7]
	yes	yes	no	31	[8]
	yes	yes	no	70	[3, 9, 10]
	yes	yes	no	300	[11]
	yes	yes	no	400	[12-14]
Electrostatic	no	yes	yes	100	[15]
Electroactive Polymer	yes	yes	no	64	[16]
Optical	yes	yes	no	10 000	[17]
Base Vibration	no	no	no	800	[18, 19]
Mechanical	yes	no	yes	500-1000	[20]
Pneumatic	yes	yes	yes	500	[21, 22]
	no	yes	yes	10 000	[23]

As can be concluded from Table 1, pneumatic artificial cilia are uniquely suitable to study the influence of different types of asymmetry on fluid flow, since all asymmetry types are reproducible and also adjustable, which is especially important in experimental investigations. This chapter will focus on pneumatically controlled artificial cilia, where two types of pneumatic cilia can be distinguished: those where passive hair like structures are implanted on top of a pneumatically actuated base membrane and those where the body of the hair like structure itself is pneumatically actuated. Both types will be described separately in the following paragraphs.

2. BASE ACTUATED PNEUMATIC CILIA

A first type of artificial pneumatic cilia consists of passive platelets that are implanted at an angle on top of a flexible membrane, as shown in Figure 1, and as reported by Rockenback et al. [21, 22, 24]. Being plate-like in form and working at a Reynolds number equal to 5, these cilia mimic the propulsion system of ctenophores [25]. Each flap stands off-centre on a thin membrane which can be pressurized or depressurized. This variation of pressure deflects the membranes changing their curvature, and consequently changing the inclination of the flaps on top. By imposing a sinusoidal pressure between -0.6 bar and 0.6 bar, the implanted plates exhibit spatial asymmetry, as can be seen on Figure 1 ‘d’. Further, by changing the rate of inflation and deflation of the membrane, temporal asymmetry can be adjusted, and as consecutive membranes can be individually controlled, metachronal asymmetry is possible. As such, this system exhibits all four types of asymmetry, where metachronal and temporal asymmetry are adjustable by tuning the pneumatic input cycle, while orientational and spatial asymmetry are determined by the production process. The flaps, supporting membranes and pneumatic connections are made out of PDMS using a soft lithography process involving two SU8 micromoulds and a post-cure deformation step to introduced the inclination. Each flap measures 500 μm high and 50 μm thick, and is located on a membrane which is 175 μm thick and 600 μm wide. The pitch between the flaps is 1000 μm. The overall design is depicted in Figure 1 ‘b’.

The performance of these base actuated plate-like cilia has been tested using experiments in water, where also the effect of orientational asymmetry and metachronal asymmetry has been studied. The influence of orientational asymmetry is quantified by using four different inclination angles of the flaps, while keeping metachronal, temporal and orientational asymmetry constant. In all cases, a constant temporal asymmetry is achieved by imposing a positive actuation pressure for 40ms (effective stroke) and a negative

actuation pressure for 103ms (recovery stroke). The symplectic metachronal asymmetry is set by having a fixed time shift of 20ms between cilia and all cilia exhibited the same spatial asymmetry, as is shown in Figure 1 ‘d’. The resulting fluid flow has been measured using Particle Image Velocimetry (PIV) and simulated using Computational Fluid Dynamics (CFD). The results of these test for flaps with an inclination angle of 45° is depicted in Figure 2 ‘a’. These figures show a positive net velocity, that is largest at the cilia tips. The influence of orientational asymmetry can be seen on Figure 2 ‘b’, where it can be seen that increasing orientational asymmetry has a positive influence on net fluid flow, shifting it from an initial negative to a positive net fluid flow.

The influence of metachronal asymmetry has been experimentally studied, by changing the time shift between actuated flaps, while keeping temporal, orientational and spatial asymmetry constant [24]. To observe the fluid flow and evaluate the velocities, particle path-lines pictures were acquired, and used to calculate mean fluid velocities. The results of changing metachrony on this mean fluid flow can be seen on Figure 3, where beating frequencies were tested of up to 5 Hz. As shown, synchronous beating leads to low mean velocities compared to when metachrony is introduced. This can be explained by the absence of a relative motion between the neighbouring walls. This relative motion squeezes fluid out of the gaps between cilia into the upper layer, above the cilia tips, where it contributes to the main flow. It is also observed that symplectic metachrony (mean fluid velocity is in the same direction as the effective stroke) causes higher velocities than antiplectic metachrony. This is in contrast to the theoretical findings for low Reynold number ciliated fluid flow of Khaderi et al. [10], that showed for low Reynolds flow an increased performance of antiplectic metachrony over symplectic metachrony. As the base actuated pneumatic cilia operate at a Reynolds number of 5, it can be concluded that inertial effects play an important role on metachronally induced fluid flow [24].

3. BODY ACTUATED PNEUMATIC CILIA

As shown above, base actuated pneumatic cilia can give clear insights in the influence of certain types of asymmetry on fluid flow. However, it is hard to distinguish the effect of the protruding cilia from the effect of the base itself. Further, the shape of the cilia remains straight throughout its stroke while cilia in nature often use a change in shape to propel fluid. This can be clearly seen in the beating pattern of natural cilia, as shown in Figure 4, where the cilia body is extended throughout the effective stroke and bended during the recovery stroke. Body actuated pneumatic cilia on the other hand try to mimic these advanced beating patterns by actuating the internal structure of the cilia itself rather than actuating the base structure. An artificial equivalent of this concept has been presented by Gorissen et al. [23], where a pneumatic bending microactuator is used as a biomimicking cilia. The artificial cilium consists of a PDMS cylinder with a length of 8 mm and a diameter of 1 mm, which has an inner cylindrical void with a diameter of 0.6 mm and an eccentricity with respect to the outer structure of 0.14 mm. Due to this eccentricity, the structure bends when the inner void is pressurized, generating the effective stroke, as can be seen on Figure 5 ‘a’. When actuated, this cilium exhibits orientational asymmetry, that can be adjusted by influencing the actuation frequency. This is shown on Figure 5 ‘b’, where it is also clear that when the cilium is actuated above its natural bandwidth, it cannot complete its entire stroke. This stroke reduction causes the mean bending deformation to increase, resulting in an increased orientational asymmetry. Further, this pneumatic cilium can exhibit temporal asymmetry, by changing the rate of inflation and deflation, and when put in an array, metachrony is adjustable by actuating the cilia with a phase difference between them. These cilia thus only lack the ability of spatial asymmetry.

In a first test, a single cilium was immersed in an ink bath and actuated at 10 Hz, as is shown on Figure 5 ‘a’. The pneumatic input signal was provided using a fast switching pneumatic valve (Festo, MH2), which was also used to actuate the cilia array where each cilia is actuated using a separate valve. Consecutive images show high Reynolds fluid propulsion in the actuation direction, which is accordance with the theoretical results of

Khaderi et al. [2]. Subsequently, the net propulsion generated by the cilia array is measured in the configuration of no metachrony, symplectic metachrony and antiplectic metachrony for duty cycles of 80% and 20% in a range of frequencies varying between 1 and 35 Hz. The results are summarized in Figure 6 ‘a’ and ‘b’. Over all frequencies, it is not possible to make concise conclusions on which type of metachrony is best or achieving fluid propulsion. This is in contrast to the conclusions with the base actuated pneumatic cilia. Below 11 Hz, in all cases a flow directed in the opposite direction of the effective strokes of the cilia is observed. However, above 11 Hz, the change in the orientational asymmetry caused by the duty cycle at 80% appears to generate a flow reversal, even though the orientation angle does not shift in sign. PIV measurements, as shown in Figure 6 ‘c’, explain these observations: generally the single cilium propels fluid in the same direction as its bending motion, but when it is placed in the array configuration, the momentum is blocked by the second proximal cilium which forces the fluid to go back over the actuated cilia and move in the opposite direction. This blockage is less pronounced when the duty cycle is 80% and the frequency is high, since in this case the second cilium is in a more bended configuration, allowing the flow to move in the same direction as the bending direction. Lastly, these tests show that for high Reynolds propulsion ($Re \approx 4000$), no spatial asymmetry is needed to achieve fluid propulsion.

4. CONCLUSION

During the previous decade, artificial cilia have been developed using a wide variety of actuation principles. Recently, new types of artificial cilia have been introduced that are using flexible pneumatic actuators to achieve propulsion, either by deforming the base of the cilia or the cilia itself. Compared to other actuation principles, these pneumatic cilia are uniquely suited to validate existing cilia propulsion theories, since these artificial cilia allow all types of asymmetry to be independently activated and adjusted in magnitude. This makes it possible to differentiate between asymmetry types and carefully analyse the contribution of each type to the overall fluid flow. Artificial pneumatic cilia are thus an important enabler to experimentally study these fascinating propulsion systems.

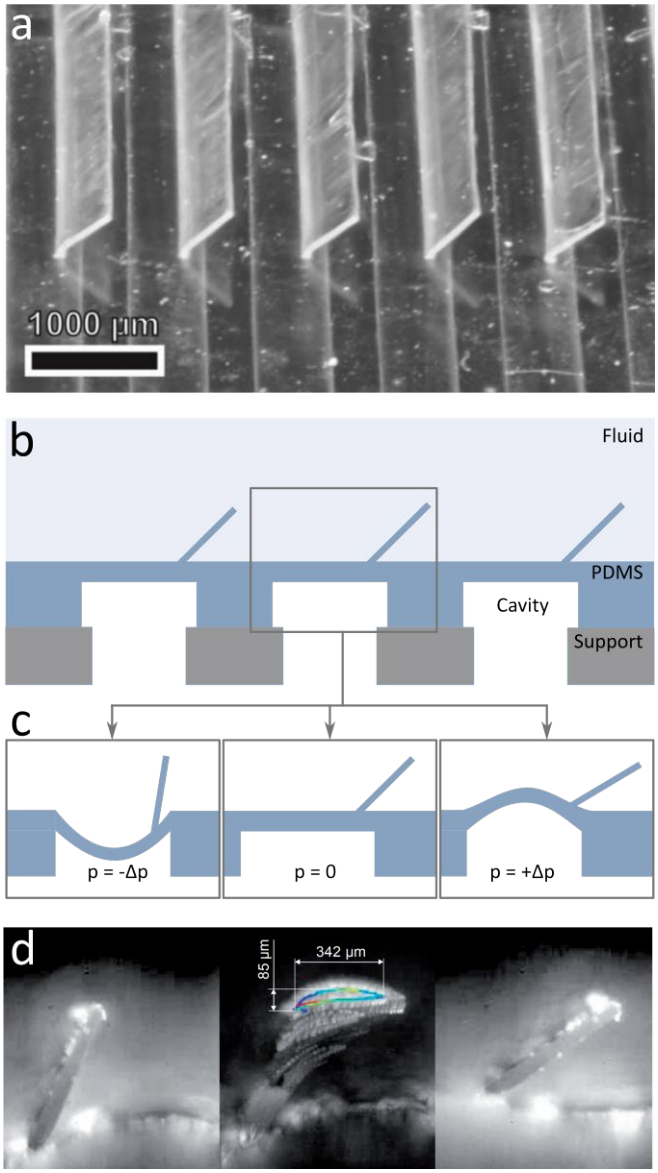

Figure 1 Schematic overview of base actuated pneumatic cilia, that in essence are tilted flaps with an inclination angle of 45°, as shown in photograph ‘a’. These tilted flaps are located on top of a deformable PDMS membrane, as can be seen on ‘c’. When actuating the cavity beneath the membrane, these plate-like cilia exhibit spatial asymmetry, as is depicted schematically in ‘c’ and using pictures in ‘d’. Pictures adapted from [21, 22].

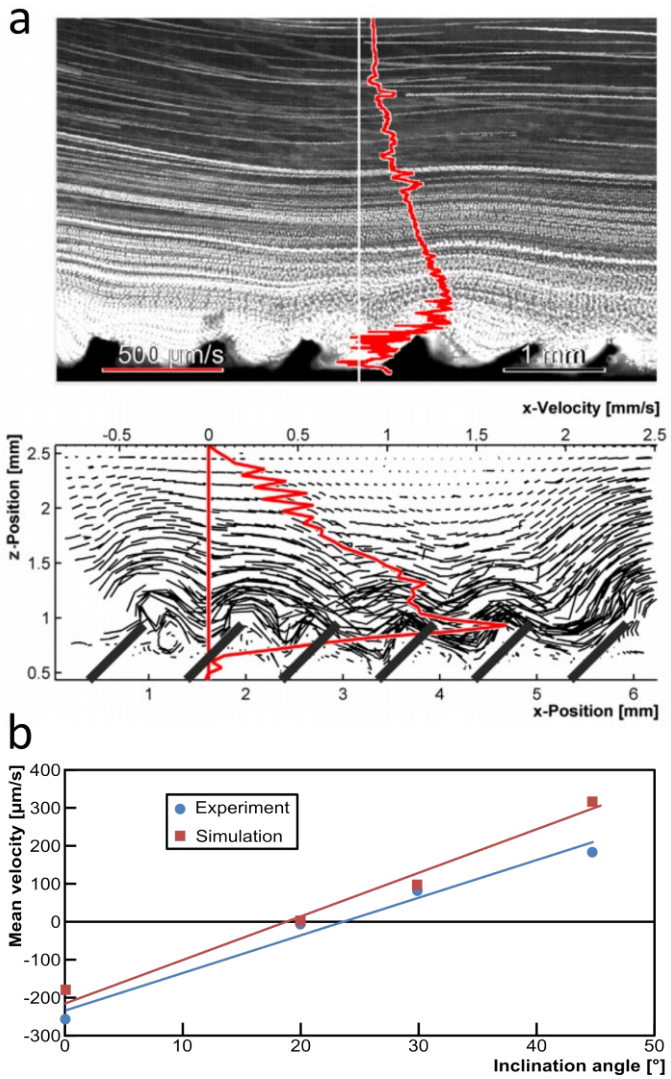

Figure 2 ‘a’: Stream profile of the transported fluid for flaps with an inclination angle of 45°. Top: experimentally obtained through PIV. Bottom: Simulated. ‘b’: Comparison of mean velocities while influencing orientational asymmetry by changing flap inclination angle. Pictures from [21]

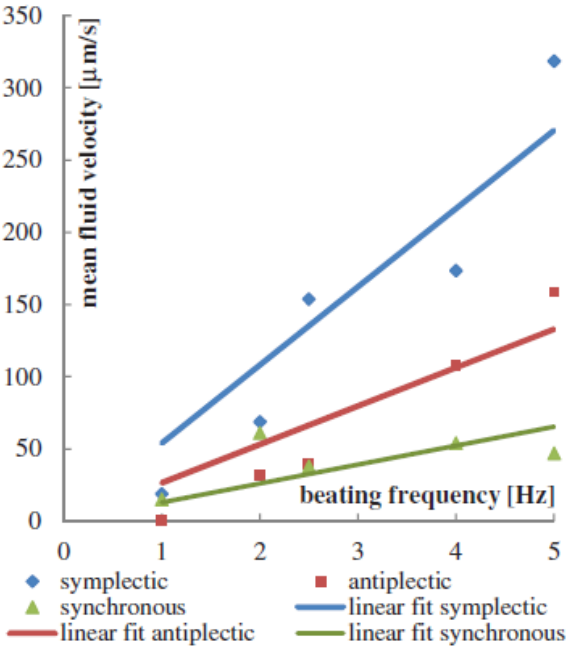

Figure 3 Influence of metachrony on mean fluid flow, for plate-like body actuated pneumatic cilia. Picture from [24]

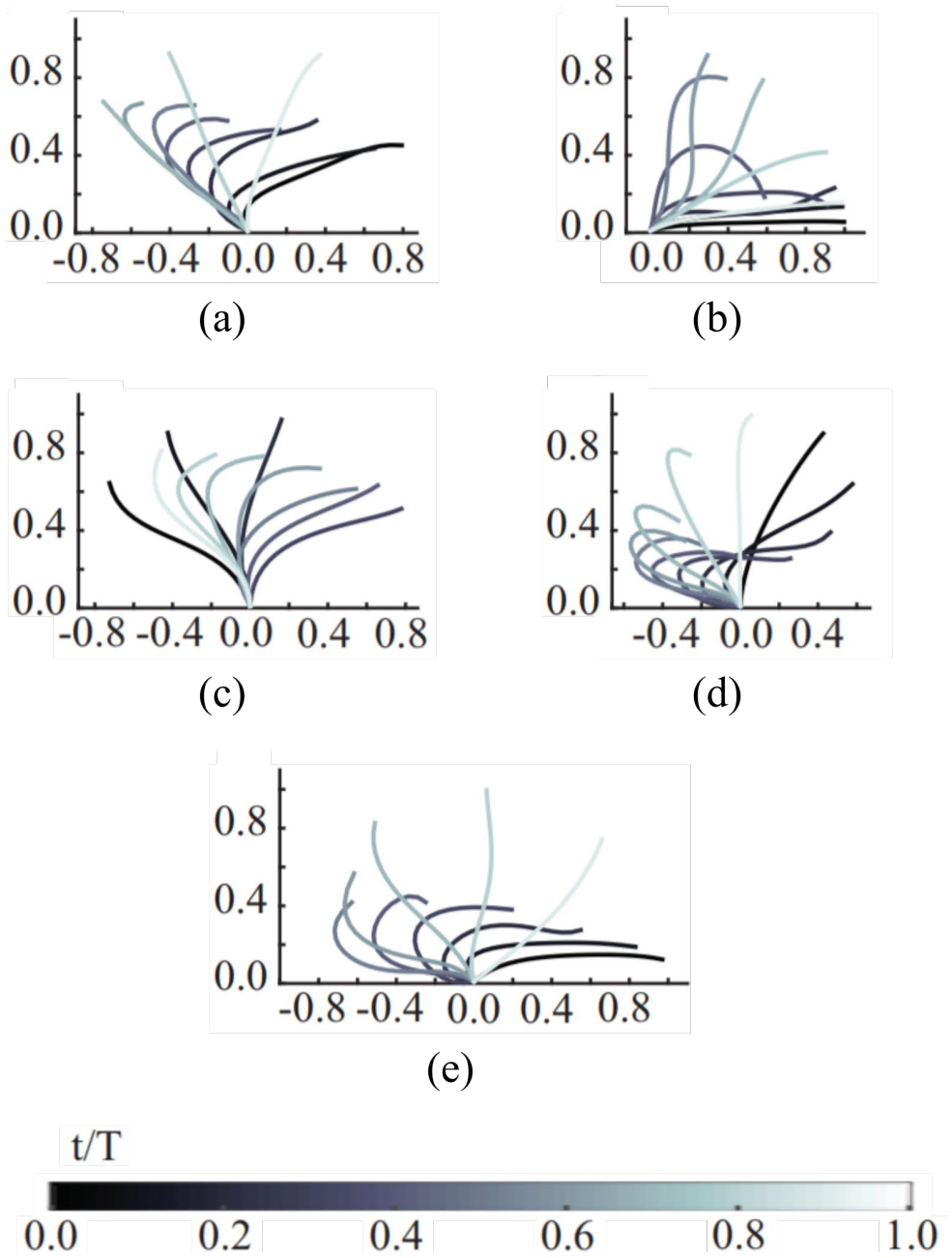

Figure 4 Beating patters of natural cilia for (a) *Paramecium*, (b) *Opalina*, (c) rabbit tracheal cilia, (d) *Sabellaria* gill, (e) *Didinium*. Figure from [26].

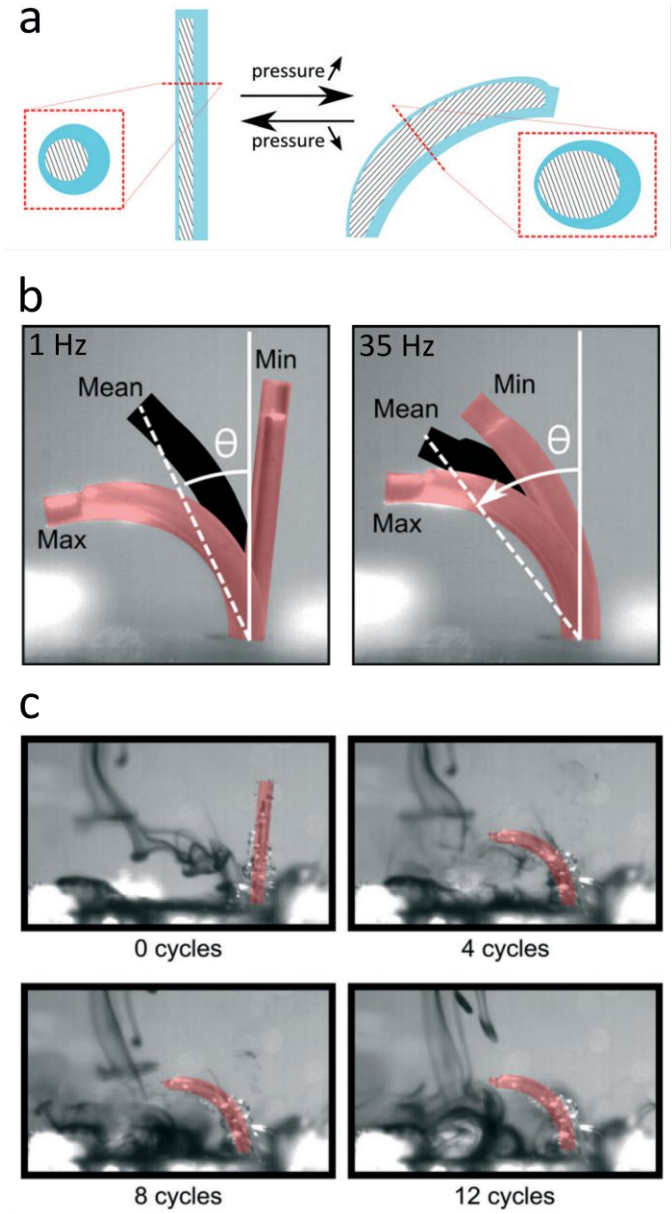

Figure 5 ‘a’: Schematic overview of the pneumatic cilia without spatial asymmetry. ‘b’: Stroke reduction that appears when the cilia is actuated at 35Hz, compared to the full stroke at 1 Hz. As the mean bending angle changes with stroke reduction, orientational asymmetry is also influenced. ‘c’: High Reynolds fluid propulsion of a single cilia, showing a net fluid flow in the bending direction. Pictures from [23].

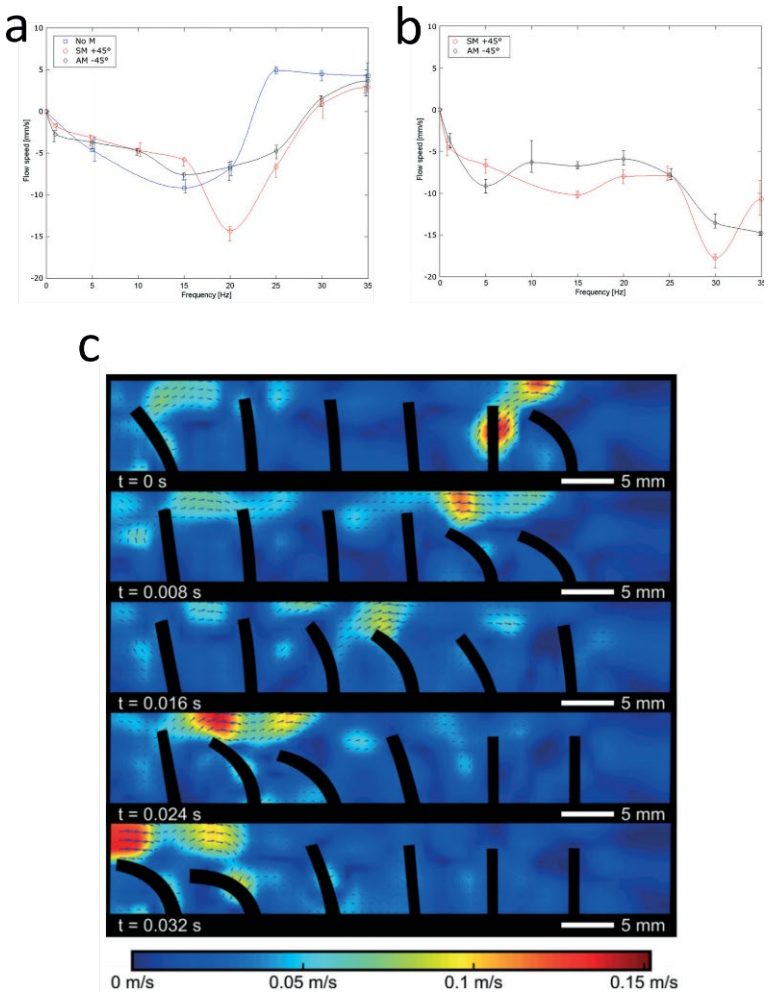

Figure 6 ‘a’:Effect of metachrony (no metachrony: No M, symplectic metachrony: SM and anitplectic metachrony: AM) on flow speed, for an actuated cilia array with duty cycle of 80% (left) and 20% (right). ‘b’: Velocity field for symplectic metachrony with frequency of 20Hz and duty cycle of 20% and phase difference of 45°, registered through PIV. Pictures from [23].

5. ACKNOWLEDGEMENTS

This book chapter has been made possible by the Fund for Scientific Research-Flanders (FWO) and the European Research Council (ERC starting grant HIENA).

6. REFERENCES

[1] E.M. Purcell, LIFE AT LOW REYNOLDS-NUMBER, American Journal of Physics 45(1) (1977) 3-11.

[2] S.N. Khaderi, M.G.H.M. Baltussen, P.D. Anderson, J.M.J. den Toonder, P.R. Onck, Breaking of symmetry in microfluidic propulsion driven by artificial cilia, Physical Review E 82(2) (2010).

[3] J. Hussong, N. Schorr, J. Belardi, O. Prucker, J. Ruehe, J. Westerweel, Experimental investigation of the flow induced by artificial cilia, Lab on a Chip 11(12) (2011) 2017-2022.

[4] C. Brennen, H. Winet, FLUID-MECHANICS OF PROPULSION BY CILIA AND FLAGELLA, Annual Review of Fluid Mechanics 9 (1977) 339-398.

[5] A.R. Shields, B.L. Fiser, B.A. Evans, M.R. Falvo, S. Washburn, R. Superfine, Biomimetic cilia arrays generate simultaneous pumping and mixing regimes, Proceedings of the National Academy of Sciences of the United States of America 107(36) (2010) 15670-15675.

[6] B.A. Evans, A.R. Shields, R.L. Carroll, S. Washburn, M.R. Falvo, R. Superfine, Magnetically actuated nanorod arrays as biomimetic cilia, Nano Letters 7(5) (2007) 1428-1434.

[7] F. Fahrni, M.W.J. Prins, L.J. van Ijzendoorn, Micro-fluidic actuation using magnetic artificial cilia, Lab on a Chip 9(23) (2009) 3413-3421.

[8] M. Vilfan, A. Potocnik, B. Kavcic, N. Osterman, I. Poberaj, A. Vilfan, D. Babic, Self-assembled artificial cilia, Proceedings of the National Academy of Sciences of the United States of America 107(5) (2010) 1844-1847.

[9] S. Khaderi, J. Hussong, J. Westerweel, J. den Toonderc, P. Onck, Fluid propulsion using magnetically-actuated artificial cilia - experiments and simulations, Rsc Advances 3(31) (2013) 12735-12742.

[10] S.N. Khaderi, C.B. Craus, J. Hussong, N. Schorr, J. Belardi, J. Westerweel, O. Prucker, J. Ruehe, J.M.J. den Toonder, P.R. Onck, Magnetically-actuated artificial cilia for microfluidic propulsion, Lab on a Chip 11(12) (2011) 2002-2010.

[11] Y. Wang, J. den Toonder, R. Cardinaels, P. Anderson, A continuous roll-pulling approach for the fabrication of magnetic artificial cilia with microfluidic pumping capability, Lab on a Chip 16(12) (2016) 2277-2286.

[12] C.Y. Chen, C.C. Hsu, K. Mani, B. Panigrahi, Hydrodynamic influences of artificial cilia beating behaviors on micromixing, Chemical Engineering and Processing 99 (2016) 33-40.

[13] C.-Y. Chen, L.-Y. Cheng, C.-C. Hsu, K. Mani, Microscale flow propulsion through bioinspired and magnetically actuated artificial cilia, Biomicrofluidics 9(3) (2015).

[14] C.Y. Chen, C.Y. Lin, Y.T. Hu, Magnetically actuated artificial cilia for optimum mixing performance in microfluidics, Lab on a Chip 13(14) (2013) 2834-2839.

[15] J. den Toonder, F. Bos, D. Broer, L. Filippini, M. Gillies, J. de Goede, T. Mol, M. Reijme, W. Talen, H. Wilderbeek, V. Khatavkar, P. Anderson, Artificial cilia for active micro-fluidic mixing, Lab on a Chip 8(4) (2008) 533-541.

[16] S. Sareh, J. Rossiter, A. Conn, K. Drescher, R.E. Goldstein, Swimming like algae: biomimetic soft artificial cilia, Journal of the Royal Society Interface 10(78) (2013).

[17] C.L. van Oosten, C.W.M. Bastiaansen, D.J. Broer, Printed artificial cilia from liquid-crystal network actuators modularly driven by light, Nature Materials 8(8) (2009) 677-682.

[18] K. Oh, B. Smith, S. Devasia, J.J. Riley, J.H. Chung, Characterization of mixing performance for bio-mimetic silicone cilia, Microfluidics and Nanofluidics 9(4-5) (2010) 645-655.

[19] K. Oh, J.-H. Chung, S. Devasia, J.J. Riley, Bio-mimetic silicone cilia for microfluidic manipulation, Lab on a Chip 9(11) (2009) 1561-1566.

[20] A. Keissner, C. Bruecker, Directional fluid transport along artificial ciliary surfaces with base-layer actuation of counter-rotating orbital beating patterns, Soft Matter 8(19) (2012) 5342-5349.

[21] A. Rockenbach, U. Schnakenberg, The influence of flap inclination angle on fluid transport at ciliated walls, Journal of Micromechanics and Microengineering 27(1) (2017).

[22] A. Rockenbach, U. Schnakenberg, Structured PDMS used as active element for a biomimetics inspired fluid transporter, Lekar a technika - Clinician and Technology 2(45) (2015) 37-41.

[23] B. Gorissen, M. de Volder, D. Reynaerts, Pneumatically-actuated artificial cilia array for biomimetic fluid propulsion, Lab on a Chip 15(22) (2015) 4348-4355.

[24] A. Rockenbach, V. Mikulich, C. Brucker, U. Schnakenberg, Fluid transport via pneumatically actuated waves on a ciliated wall, Journal of Micromechanics and Microengineering 25(12) (2015).

[25] A. Dauptain, J. Favier, A. Bottaro, Hydrodynamics of ciliary propulsion, Journal of Fluids and Structures 24(8) (2008) 1156-1165.

[26] H.L. Guo, E. Kanso, Evaluating efficiency and robustness in cilia design, Physical Review E 93(3) (2016).